

Luminosity Loss due to Kicks and Mismatch from radio-frequency breakdown in a Linear Collider

V. Ziemann

Department of Physics and Astronomy
Uppsala University, Uppsala, Sweden

June 21, 2017

Abstract

We calculate the geometric luminosity loss caused by filamentation of transverse kicks, upright and skew quadrupolar errors due to discharges, so-called RF-breakdown, in the acceleration structures of a Linear Collider.

1 Introduction

The required high accelerating gradient of 100 MV/m in the CLIC [1] linear accelerator causes surface electric fields which are in excess of 200 MV/m and this occasionally causes discharges, so-called RF breakdown, in which a plasma is generated leading to the ejection of electrons and ions from accelerating structures [2]. Moreover, the plasma effectively generates an electric short circuit in the structure that causes the RF fields to be reflected [3]. Recently, we analyzed the effect of these discharges on the accelerated beam [4] and found that the discharges cause a transverse kick of the beam as well as changing the beam size and therefore causing a betatron mismatch.

In case that a discharge occurs early in the linear accelerator at lower energies we expect that the finite momentum spread of the beam will cause full filamentation [6] of the displacement or betatron mismatch, because particles kicked or otherwise displaced to different amplitudes from those of a matched and centered beam will start betatron oscillations at their amplitudes and eventually will be spread out over a matched phase space ellipse, which will cause the emittance to grow and the distribution of particles in phase space to change. This effect is normally considered as phase space dilution due to injection mismatch in storage rings, but the same concepts can be applied to evaluate the effect of mismatch and transverse kicks on the luminosity in linear colliders.

In order to calculate the reduction of the luminosity we need to take the detailed shape of the distribution after filamentation into account, considering rms beam sizes only is insufficient, because the final distributions are sometimes significantly different from Gaussian [5].

In the remainder of this report we first introduce the relevant beam dynamics concepts that are needed for to calculate these non-Gaussian distributions. We start by investigating the the luminosity loss due to a transverse kick in one phase space dimension and then progress to the consequence of betatron mismatch and finally consider the result of a localized skew quadrupolar error and finally summarize our findings in the conclusions.

2 Normalized Phase Space

In order to simplify the algebra, we start by introducing normalized phase space (\tilde{x}, \tilde{x}') , denoted by a tilde. It is related to normal transverse phase space coordinates (x, x') in an accelerator by the transformation

$$\begin{pmatrix} x \\ x' \end{pmatrix} = \begin{pmatrix} \sqrt{\beta} & 0 \\ -\alpha/\sqrt{\beta} & 1/\sqrt{\beta} \end{pmatrix} \begin{pmatrix} \tilde{x} \\ \tilde{x}' \end{pmatrix} = \mathcal{A} \begin{pmatrix} \tilde{x} \\ \tilde{x}' \end{pmatrix} \quad (1)$$

where β and α are the normal Twiss parameters at a given location in the magnet lattice. Here we also introduced the abbreviation \mathcal{A} for the matrix appearing in the previous equation.

In all our analysis we assume that the initial beam distribution is Gaussian in all phase space coordinates. In particular, the matrix of central second moments $\bar{\sigma}$, the so-called sigma matrix, can be expressed in terms of the matrix \mathcal{A} and the emittance ε as

$$\bar{\sigma} = \varepsilon \bar{\mathcal{A}} \bar{\mathcal{A}}^t = \varepsilon \begin{pmatrix} \bar{\beta} & -\bar{\alpha} \\ -\bar{\alpha} & \bar{\gamma} \end{pmatrix} \quad (2)$$

where $\bar{\mathcal{A}}^t$ denotes the transpose of $\bar{\mathcal{A}}$ and with the condition $\bar{\gamma} = (1 + \bar{\alpha}^2)/\bar{\beta}$. Here the quantities with a bar denote those of the incoming beam. If the incoming beam is matched, we have $\bar{\beta} = \beta$ and $\bar{\alpha} = \alpha$.

Propagating beam particles through a beam line consisting of linear elements is accomplished by transfer matrices R which can also be represented using the matrices \mathcal{A} and normal 2×2 rotation matrices

$$R = \mathcal{A}_f \mathcal{O}_\mu \mathcal{A}_i^{-1} \quad \text{with} \quad \mathcal{O}_\mu = \begin{pmatrix} \cos \mu & \sin \mu \\ -\sin \mu & \cos \mu \end{pmatrix} \quad (3)$$

and \mathcal{A}_i contains the Twiss parameters at the initial location of the beam line section represented by R and \mathcal{A}_f those of the final location. The betatron phase advance is denoted by μ .

As a trivial example to illustrate the usefulness of the formalism we consider a periodic system with $\mathcal{A}_f = \mathcal{A}_i$ and a matched beam where the initial beam matrix σ_i is constructed from the same \mathcal{A}_i according to eq. 2. In that case we calculate the final beam matrix σ_f from

$$\sigma_f = R\sigma_i R^t = \mathcal{A}_i \mathcal{O} \mathcal{A}_i^{-1} \varepsilon \mathcal{A}_i \mathcal{A}_i^t \left(\mathcal{A}_i \mathcal{O} \mathcal{A}_i^{-1} \right)^t = \varepsilon \mathcal{A}_i \mathcal{A}_i^t = \sigma_i \quad (4)$$

and find that it is equal to the initial beam matrix σ_i , as expected.

The sigma matrix is a convenient tool to propagate the beam through a linear array of beam line elements, but the beam is always assumed to be Gaussian. In order to be able to handle more general distributions we start by considering an initial multi-variate Gaussian particle distribution $\psi(x, x')$ in the particle coordinates $(x_1, x_2) = (x, x')$ which is given by

$$\psi(x, x') = \frac{1}{2\pi\sqrt{\det \sigma}} \exp \left[-\frac{1}{2} \sum_{i=1}^2 \sum_{j=1}^2 \sigma_{ij}^{-1} x_i x_j \right]. \quad (5)$$

This distribution is normalized to unity and characterized by the sigma matrix σ . This expression can be trivially generalized to more phase space coordinates. Note that we can write the inverse of a sigma matrix, using eq. 2 as

$$\sigma^{-1} = \frac{1}{\varepsilon} \left(\mathcal{A}^t \right)^{-1} \mathcal{A}^{-1} = \frac{1}{\varepsilon} \begin{pmatrix} \gamma & \alpha \\ \alpha & \beta \end{pmatrix} \quad (6)$$

which will prove convenient later on.

Any distribution function $\Psi_X(\vec{X})$ depending on variables \vec{X} can be transformed to new variables $\vec{Y} = f(\vec{X})$ in the following way

$$\Psi_Y(\vec{Y}) = \frac{1}{|J_f(\vec{Y}, \vec{X})|} \Psi_X \left(f^{-1}(\vec{Y}) \right) \quad (7)$$

where Ψ_Y depends on the new variables \vec{Y} . The inverse of the variable transformation f is denoted by f^{-1} and $J_f(\vec{Y}, \vec{X})$ refers to the Jacobian of f . In the particular case where the variable transformation f stems from a linear transformation described by matrix R the distribution function $\psi(x, x')$ in eq. 5 is transformed to new variables $(y, y')^t = R(x, x')^t$ by simply replacing the sigma matrix in eq. 5 by the one transformed to the new coordinates, given by the familiar expression $R\sigma R^t$.

In the case where we change the variables of the distribution function to those of normalized phase space using eq. 1 we find

$$\psi(\tilde{x}, \tilde{x}') = \frac{1}{2\pi\varepsilon} \exp \left[-\frac{\tilde{x}^2 + \tilde{x}'^2}{2\varepsilon} \right] \quad (8)$$

which describes a rotationally symmetric Gaussian in the two phase space variables \tilde{x} and \tilde{x}' . Introducing action and angle variables (J, ϕ) in normalized phase space by

$$\tilde{x} = \sqrt{2J} \cos \phi \quad \text{and} \quad \tilde{x}' = \sqrt{2J} \sin \phi \quad (9)$$

we can write the previous equation in the form

$$\psi(J, \phi) = \frac{1}{2\pi\varepsilon} e^{-J/\varepsilon} \quad (10)$$

where we have used the fact that the Jacobian of the transformation from \tilde{x} and \tilde{x}' to J and ϕ has unit Jacobian and the expression for the matched beam in action-angle variables in normalized phase space is independent of the angle variable. Note that propagation with a betatron phase advance μ increases the phase variable ϕ by μ and leaves the action variable unaffected, the distribution in eq. 10 remains the same.

We start by considering the effect of transverse kicks on the luminosity in the following section.

3 Transverse Kick

In this section we address the effect of a localized transverse kick that completely filaments on its journey down the linear accelerator. We assume that the initial beam is matched to the beam line, but all particles of the distribution receive a transverse kick of magnitude θ which changes the particle coordinates from (x, x') to $(x, x' - \theta)$. Translated to normalized phase space this kick leads to the variable transformation from (\tilde{x}, \tilde{x}') to $(\tilde{x}, \tilde{x}' - \sqrt{\beta}\theta)$. Applying this coordinate transformation to the matched beam given by eq. 8 we obtain the distribution for the kicked beam

$$\psi_k(\tilde{x}, \tilde{x}') = \frac{1}{2\pi\varepsilon} \exp \left[-\frac{\tilde{x}^2 + (\tilde{x}' - \sqrt{\beta}\theta)^2}{2\varepsilon} \right] \quad (11)$$

and introducing the action angle variables given in eq. 9 arrive at

$$\psi_k(J, \phi) = \frac{1}{2\pi\varepsilon} \exp \left[-\frac{J}{\varepsilon} - \frac{\beta\theta^2}{2\varepsilon} \right] \exp \left[\frac{\theta\sqrt{2J\beta} \sin \phi}{\varepsilon} \right] \quad (12)$$

which reduces to the un-kicked distribution in eq. 10 in the case that $\theta = 0$.

Equation 12 describes the distribution immediately after the kick. During its further passage down the linear accelerator we assume that the beam filaments completely, which means that the particles located at a given angle ϕ are evenly distributed over all phase angles, which amounts to averaging the kicked distribution $\psi_k(J, \phi)$ in eq. 12 over all angles ϕ to arrive at the distribution $\psi_f(J)$ after

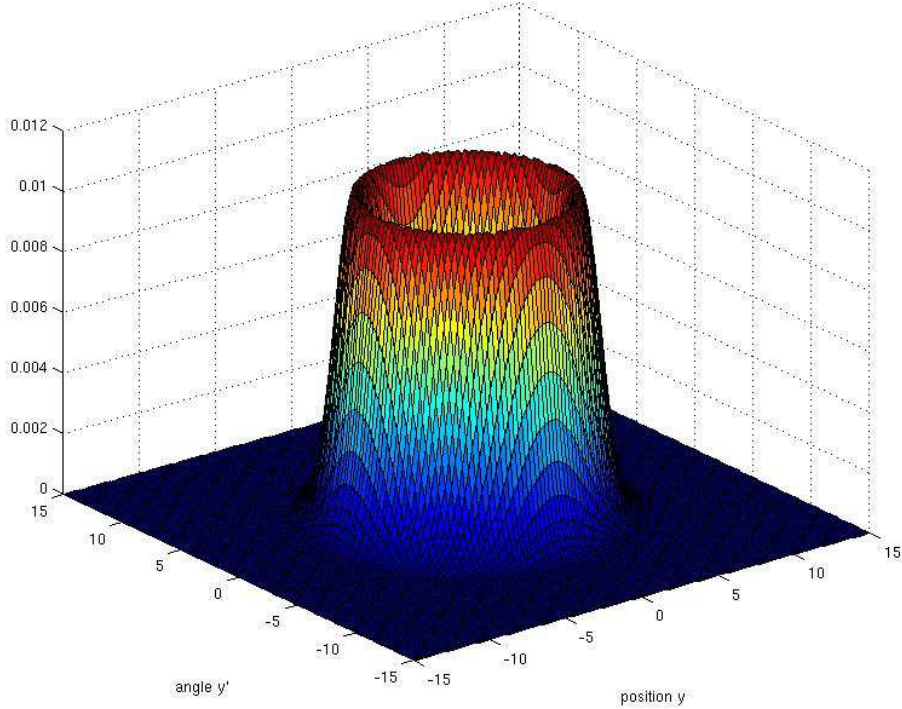


Figure 1: Kicked distribution in normalized phase space after filamentation. The kick amplitude corresponds to 6 times the angular divergence.

filamentation, given by

$$\psi_f(J) = \frac{1}{2\pi} \int_0^{2\pi} \psi_k(J, \phi) d\phi = \frac{1}{2\pi\varepsilon} \exp\left[-\frac{J}{\varepsilon} - \frac{\beta\theta^2}{2\varepsilon}\right] I_0\left(\frac{\sqrt{2J\beta\theta}}{\varepsilon}\right) \quad (13)$$

where we have used the integral representation of the modified Bessel function $I_0(z)$ given by equation 9.6.16 in Ref. [7] to evaluate the integral over ϕ . This expression is similar to the one found for example in ref. [8].

In Fig. 1 we show the kicked distribution in normalized phase space after full filamentation. The kick amplitude used in this plot was $\theta = 6\sqrt{\varepsilon/\beta}$ or six times the angular divergence at the location where the kick is applied. We observe that the distribution is rotationally invariant and has an annular shape with a hole in the center, which is what we intuitively expect. The distribution in the transverse coordinate \tilde{x} is given by projecting the two-dimensional distribution shown in Fig. 1 onto the spatial axis, which is equivalent to integrating over the angle variable \tilde{x}' . We show the result of the projection for different kick amplitudes in Fig. 2. For $\theta = 0$ we recover the Gaussian with unit width. For increasing kick

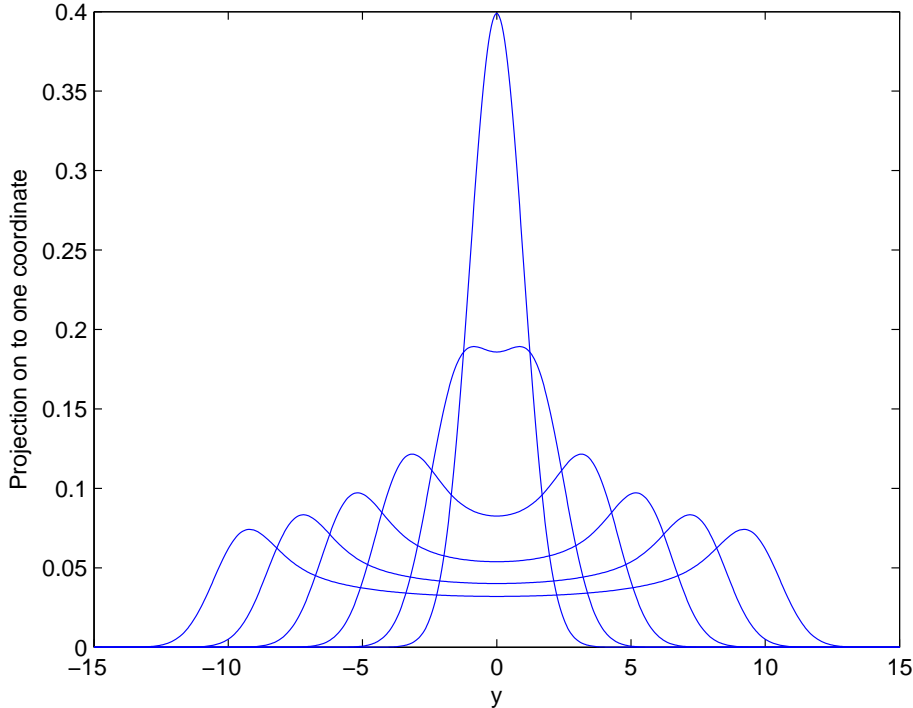


Figure 2: Projection of the fully filamented distribution onto the \tilde{x} -axis for normalized kick amplitudes of $\theta/\sqrt{\varepsilon/\beta}$ equal to $0, 2, \dots, 10$ and $\varepsilon = 1$ mrad.

amplitude we see that the peak value of the distribution gets smaller and there are two separate peaks with a reduced particle density in-between.

In order to calculate the luminosity we need to determine the transverse spatial distribution at the interaction point, which is given by the the projection of the distribution in normalized phase space, as shown in Fig. 2, mapped back into real space. But this is accomplished by multiplying the \tilde{x} axis by $\sqrt{\beta_0}$ where β_0 is the beta function at the interaction point. But since this implies rescaling the axes we might as well calculate the relative luminosity loss by using normalized phase space coordinates throughout.

We estimate the detrimental effect of the kicks on the luminosity by calculating the reduction in geometric overlap of the kicked beam with the counter-propagating beam. This approximation is valid as long as no strong beam-beam enhancement due to strong focusing of one beam on the other which results in a strong pinch effect is present. Here the geometric overlap may serve as a qualitative measure of how significant the luminosity reduction is. In a parameter regime with strong pinch effect, it can be stronger.

In the present discussion we assume that the beam line is uncoupled the kick

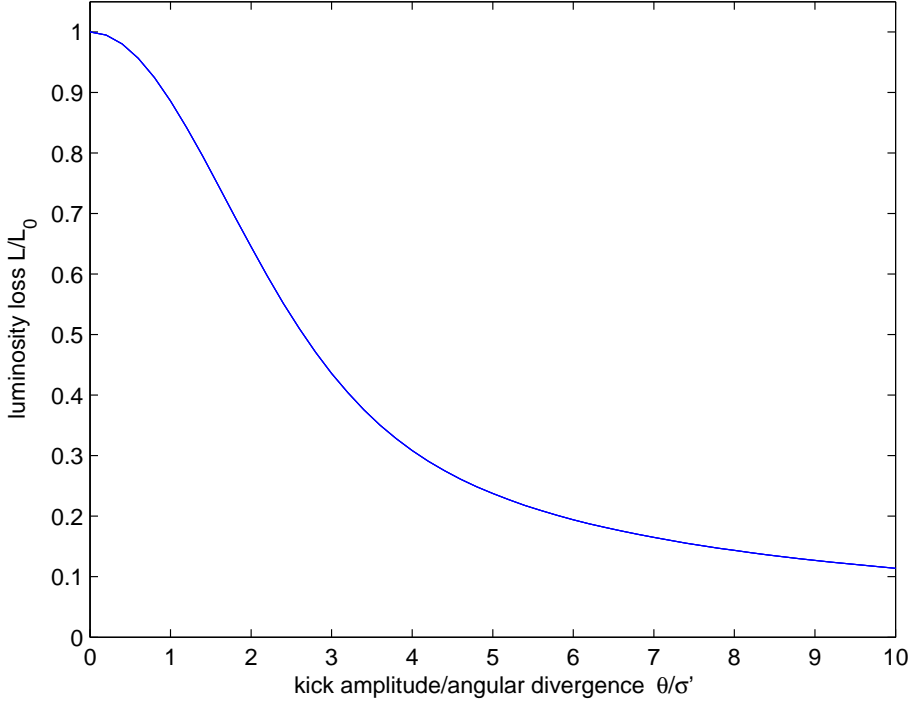


Figure 3: The relative luminosity loss as a function of the kick amplitude. Note that the loss is calculated as the geometric overlap only.

only affects the beam size in one plane and leaves the other unaffected. Thus we can calculate the luminosity loss due to fully filamented kicks by calculating the following integral

$$\mathcal{L}(\theta) = \frac{1}{\sqrt{2\pi\varepsilon}} \int_{-\infty}^{\infty} e^{-\tilde{x}^2/2\varepsilon} \left[\frac{1}{2\pi\varepsilon} \int_{-\infty}^{\infty} \psi_f \left(\sqrt{(\tilde{x}^2 + \tilde{x}'^2)/\varepsilon} \right) d\tilde{x}' \right] d\tilde{x} \quad (14)$$

where ψ_f is given by eq. 13 with the action variable J substituted by $J = (\tilde{x}^2 + \tilde{x}'^2)/2$ such that the square bracket is the projection of the filamented distribution onto the space coordinate. The second integral over \tilde{x} , weighted with the spatial distribution of the counter-propagating beam then results in the luminosity loss. This integral we evaluated numerically.

In Fig. 3 we show the luminosity, normalized to the value \mathcal{L}_0 at kick angle $\theta = 0$ as a function of the kick angle in units of the angular divergence at the location where the kick occurs. We find that small kick angles of magnitude less than one sigma causes a luminosity reduction on the order of 10%. We also note that already for a kick of two-sigma magnitude almost halves the luminosity and are clearly very detrimental. We also observe that even for very large kicks of

ten sigma amplitude the filamentation causes some of the particles to be near the center of the beam line where they can interact with the counter-propagating beam, albeit at a significant lower rate. The luminosity at ten sigma is only about 10% of the value when beams of equal size meet.

We now turn to the analysis of the effect of a betatron mismatch, for instance due to quadrupolar errors, on the luminosity.

4 Betatron Mismatch

In the case of a betatron mismatch the incoming beam has Twiss parameters different from those of the matched beam. This implies that the incoming distribution is not rotationally invariant and filamentation will cause the beam size in general to grow from the initial one. We start by simply considering the emittance growth. This is easily done by calculating the final sigma matrix

$$\sigma_f = R\sigma R^t = (\mathcal{A}\mathcal{O}\mathcal{A}^{-1})\varepsilon(\bar{\mathcal{A}}\bar{\mathcal{A}}^t)(\mathcal{A}\mathcal{O}\mathcal{A}^{-1})^t. \quad (15)$$

Observe that the transfer matrix R is based on the matched Twiss parameters through the matrix \mathcal{A} whereas the incoming beam is based on different Twiss parameters $\bar{\beta}$ and $\bar{\alpha}$ that define the matrix $\bar{\mathcal{A}}$. Explicitely multiplying out the matrices we find

$$\sigma_f = \varepsilon\mathcal{A}\mathcal{O}\begin{pmatrix} \frac{\bar{\beta}}{\beta} & \alpha\frac{\bar{\beta}}{\beta} - \bar{\alpha} \\ \alpha\frac{\bar{\beta}}{\beta} - \bar{\alpha} & \alpha^2\frac{\bar{\beta}}{\beta} - 2\alpha\bar{\alpha} + \bar{\gamma}\beta \end{pmatrix}\mathcal{O}^t(\mathcal{A}^{-1})^t. \quad (16)$$

Again, performing the multiplication with the matrices \mathcal{O} results in a 2×2 matrix that contains terms with cosine and sine of the phases $\phi = \mu$ and filamentation corresponds to averaging over these phases in the range 0 to 2π causes the terms with $\cos^2 \phi$ and $\sin^2 \phi$ to be replaced by their average of 1/2 and terms $\sin \phi \cos \phi$ to be replaced by zero. These simple but lengthy calculations finally lead to the final sigma matrix σ_f averaged over the phases

$$\langle \sigma_f \rangle_\phi = \varepsilon\mathcal{A}\mathcal{A}^t B_{mag} \quad (17)$$

with the conventional definition of the emittance growth factor due to betatron mismatch B_{mag} given by [9]

$$B_{mag} = \frac{1}{2} \left[\frac{\bar{\beta}}{\beta} + \alpha^2 \frac{\bar{\beta}}{\beta} - 2\alpha\bar{\alpha} + \bar{\gamma}\beta \right] = \frac{1}{2} \left[\left(\frac{\bar{\beta}}{\beta} + \frac{\beta}{\bar{\beta}} \right) + \beta\bar{\beta} \left(\frac{\bar{\alpha}}{\bar{\beta}} - \frac{\alpha}{\beta} \right)^2 \right]. \quad (18)$$

Equation 17 shows that the final beam has a sigma matrix given by the Twiss parameters of the matched beam, but an emittance that is given by the initial emittance ε multiplied by the growth factor B_{mag} . For a matched beam B_{mag} is unity.

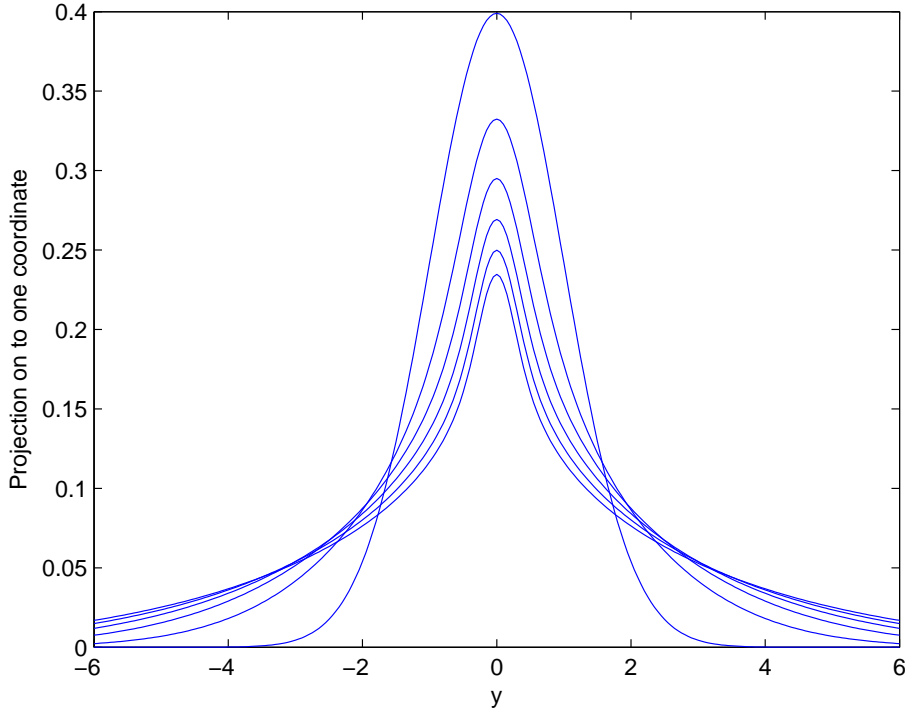


Figure 4: Transverse distribution after filamentation of a mismatched beam characterized by $B_{mag} = 1, 3, \dots, 11$.

The discussion so far only considered the sigma matrix and consequently only rms properties of the beam distribution. We will drop that restriction now and calculate the distribution after filamentation. To this end we consider the initial mismatched beam distribution given by

$$\begin{aligned} \psi(x, x') &= \frac{1}{2\pi\varepsilon} \exp \left[-\frac{1}{2}(x, x') \bar{\sigma}^{-1} \begin{pmatrix} x \\ x' \end{pmatrix} \right] \\ &= \frac{1}{2\pi\varepsilon} \exp \left[-\frac{1}{2\varepsilon}(x, x') (\bar{\mathcal{A}}\bar{\mathcal{A}}^t)^{-1} \begin{pmatrix} x \\ x' \end{pmatrix} \right] \end{aligned} \quad (19)$$

with the initial beam matrix $\bar{\sigma}$ given by eq. 2. We now apply the same method as in the previous section and introduce variables of normalized phase space through eq. 1. Since the Jacobian of that transformation is unity we can simply re-express the variables in the exponent and arrive at the distribution function in the variables \tilde{x} and \tilde{x}'

$$\psi(\tilde{x}, \tilde{x}') = \frac{1}{2\pi\varepsilon} \exp \left[-\frac{1}{2\varepsilon}(\tilde{x}, \tilde{x}') \mathcal{A}^t (\bar{\mathcal{A}}^t)^{-1} \bar{\mathcal{A}}^{-1} \mathcal{A} \begin{pmatrix} \tilde{x} \\ \tilde{x}' \end{pmatrix} \right]. \quad (20)$$

The product of the four matrices \mathcal{A} in the exponent leads to

$$\mathcal{A}^t (\bar{\mathcal{A}}^t)^{-1} \bar{\mathcal{A}}^{-1} \mathcal{A} = \begin{pmatrix} c & b \\ b & a \end{pmatrix} = \begin{pmatrix} \frac{\bar{\beta}}{\beta} + \bar{\alpha}^2 \frac{\beta}{\bar{\beta}} - 2\alpha\bar{\alpha} + \alpha^2 \frac{\bar{\beta}}{\beta} & \bar{\alpha} - \alpha \frac{\bar{\beta}}{\beta} \\ \bar{\alpha} - \alpha \frac{\bar{\beta}}{\beta} & \frac{\bar{\beta}}{\beta} \end{pmatrix} \quad (21)$$

and the distribution function can be expressed as

$$\psi(\tilde{x}, \tilde{x}') = \frac{1}{2\pi\varepsilon} \exp \left[-\frac{c\tilde{x}^2 + 2b\tilde{x}\tilde{x}' + a\tilde{x}'^2}{2\varepsilon} \right]. \quad (22)$$

Rewriting the distribution equation in terms of action-angle variables using eq. 9 we obtain

$$\psi(J, \phi) = \frac{1}{2\pi\varepsilon} \exp \left[-\frac{J \{ (c+a) + (c-a) \cos(2\phi) + 2b \sin(2\phi) \}}{2\varepsilon} \right] \quad (23)$$

which can be simplified to

$$\psi(J, \phi) = \frac{1}{2\pi\varepsilon} \exp \left[-\frac{J}{2\varepsilon} \left\{ (c+a) + \sqrt{(c-a)^2 + 4b^2} \cos(2\phi - \delta) \right\} \right] \quad (24)$$

by introducing

$$\tan \delta = \frac{2b}{c-a} \quad (25)$$

which has the advantage that only a single trigonometric function appears in the exponent and this aids evaluating the average over the angle variable we need to perform in order to calculate the fully filamented distribution

$$\begin{aligned} \psi_f(J) &= \frac{1}{2\pi} \int_0^{2\pi} \psi(J, \phi) d\phi \\ &= \frac{e^{-J(a+c)/2\varepsilon}}{2\pi\varepsilon} \frac{1}{2\pi} \int_0^{2\pi} \exp \left[-\frac{J \sqrt{(c-a)^2 + 4b^2}}{2\varepsilon} \cos(2\phi - \delta) \right] \\ &= \frac{e^{-J(a+c)/2\varepsilon}}{2\pi\varepsilon} I_0 \left(\frac{J \sqrt{(c-a)^2 + 4b^2}}{2\varepsilon} \right) \end{aligned} \quad (26)$$

where we have, again, used the integral representation of the modified Bessel function I_0 from ref. [7]. In fact, we can express the factors a, b, c to more commonly used quantities, by observing that

$$\begin{aligned} \frac{a+c}{2} &= \frac{1}{2} \left[\frac{\bar{\beta}}{\beta} + \frac{\beta}{\bar{\beta}} + \bar{\alpha}^2 \frac{\beta}{\bar{\beta}} - 2\alpha\bar{\alpha} + \alpha^2 \frac{\bar{\beta}}{\beta} \right] = B_{mag} \\ (c-a)^2 + 4b^2 &= (a+c)^2 - 4(ac - b^2) = 4(B_{mag}^2 - 1) \end{aligned} \quad (27)$$

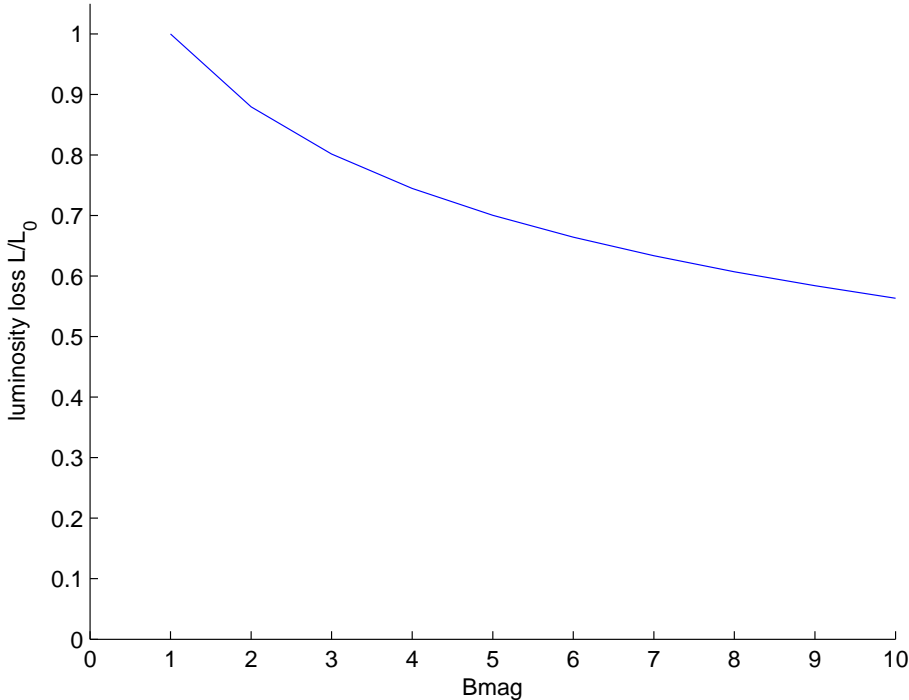


Figure 5: The relative reduction of the luminosity as a function of the betatron mismatch parameter B_{mag} .

where we note that $ac - b^2 = 1$ is the determinant of the four matrices \mathcal{A} each having unity determinant. This allows us to write the filamented distribution as

$$\psi_f(J) = \frac{1}{2\pi\varepsilon} e^{-B_{mag}J/\varepsilon} I_0 \left(\frac{J}{\varepsilon} \sqrt{B_{mag}^2 - 1} \right) \quad (28)$$

which coincides with the expression derived in ref. [5].

Similar to the previous section we now calculate the spatial distribution by re-introducing normalized phase space variable through $J = (\tilde{x}^2 + \tilde{x}'^2)/2$ in the previous equation and integrate over the angle variable \tilde{x}' . We do this integral numerically for different mismatch parameter B_{mag} and show the resulting distributions in Fig. 4. There we note that the peak intensity in the center drops with increasing B_{mag} and that the tails are increasingly populated.

Since there are less particles in the tail we also expect a reduced luminosity that we calculate in the same way as before by averaging the distribution in Fig. 4 with that of the counter-propagating beam that is assumed matched and show the result in Fig. 5. A mismatch parameter $B_{mag} = 2$ approximately causes a 10% loss of luminosity.

It is instructive to relate the mismatch parameter to an integrated quadrupole gradient error that is characterized by its focal length f . We calculate the beam matrix after the quadrupole error $\bar{\sigma}$ and compare it to the beam matrix σ that had not experienced the quadrupole error. For $\bar{\sigma}$ we have

$$\varepsilon \begin{pmatrix} \bar{\beta} & -\bar{\alpha} \\ -\bar{\alpha} & \bar{\gamma} \end{pmatrix} = \begin{pmatrix} 1 & 0 \\ -1/f & 1 \end{pmatrix} \varepsilon \begin{pmatrix} \beta & -\alpha \\ -\alpha & \gamma \end{pmatrix} \begin{pmatrix} 1 & -1/f \\ 0 & 1 \end{pmatrix}. \quad (29)$$

Evaluating the matrix multiplications we find

$$\bar{\beta} = \beta \quad \text{and} \quad \bar{\alpha} = \alpha + \frac{\beta}{f} \quad (30)$$

and inserting $\bar{\beta}$ and $\bar{\alpha}$ into the expression for B_{mag} in eq. 18 we find that a localized quadrupole error causes a beta mismatch of

$$B_{mag} = 1 + \frac{\beta^2}{2f^2}. \quad (31)$$

If an integrated quadrupole error $k_2l = 1/f$ has such a strength that the focal length is half the beta function at that location, it causes a doubling of the emittance after filamentation, but that is a rather strong quadrupole error.

5 Mismatch due to a Skew Quadrupole

We now investigate the filamentation from a thin skew quadrupolar error and derive the loss of luminosity as characterized by the geometric overlap, as before. We start by only calculating the emittance growth due to filamentation at the final point, the interaction point, of the beam line that is caused by the skew quadrupole.

The transfer matrix S of a thin skew quadrupole with focal length f is given by

$$S = \begin{pmatrix} 1 & 0 & 0 & 0 \\ 0 & 1 & 1/f & 0 \\ 0 & 0 & 1 & 0 \\ 1/f & 0 & 0 & 1 \end{pmatrix}. \quad (32)$$

We now assume that an uncoupled beam characterized by the 4×4 beam matrix

$$\bar{\sigma} = \begin{pmatrix} \sigma_x & 0_2 \\ 0_2 & \sigma_y \end{pmatrix}. \quad (33)$$

where 0_2 is the 2×2 matrix containing zeros, only and σ_x and σ_y are 2×2 beam matrices as given in eq. 2. Furthermore we assume that it describes the matched

beam. Propagating the matched beam $\bar{\sigma}$ through the skew quadrupoles we arrive at

$$\hat{\sigma} = S\bar{\sigma}S^t = \begin{pmatrix} 1_2 & Q \\ Q & 1_2 \end{pmatrix} \begin{pmatrix} \sigma_x & 0_2 \\ 0_2 & \sigma_y \end{pmatrix} \begin{pmatrix} 1_2 & Q^t \\ Q^t & 1_2 \end{pmatrix} \quad (34)$$

where 1_2 is the two-dimensional unit matrix, 0_2 the 2×2 zero-matrix, and Q is given by

$$Q = \begin{pmatrix} 0 & 0 \\ 1/f & 0 \end{pmatrix}. \quad (35)$$

Evaluating the matrix products we find

$$\hat{\sigma} = \begin{pmatrix} \sigma_x + Q\sigma_yQ^t & \sigma_xQ^t + Q\sigma_y \\ Q\sigma_x + \sigma_yQ^t & \sigma_y + Q\sigma_xQ^t \end{pmatrix}. \quad (36)$$

This expression is the sigma matrix of a matched beam after it had passed the skew quadrupole. In order to find the beam matrix at the interaction point we need to propagate it with the 4×4 transfer matrix \bar{R} given in terms of the matched beta functions and phase advance as given in eq. 3 for the horizontal and vertical plane

$$\bar{R} = \begin{pmatrix} \mathcal{A}_x\mathcal{O}_x\mathcal{A}_x^{-1} & 0_2 \\ 0_2 & \mathcal{A}_y\mathcal{O}_y\mathcal{A}_y^{-1} \end{pmatrix}. \quad (37)$$

The final 4×4 beam matrix at the interaction point $\tilde{\sigma}$ is then given by

$$\tilde{\sigma} = R\hat{\sigma}S^tR^t = \begin{pmatrix} \tilde{\sigma}_x & \text{linear in } \mathcal{O}_x \text{ and } \mathcal{O}_y \\ \text{linear in } \mathcal{O}_x \text{ and } \mathcal{O}_y & \tilde{\sigma}_y \end{pmatrix} \quad (38)$$

with

$$\begin{aligned} \tilde{\sigma}_x &= \sigma_x + (\mathcal{A}_x\mathcal{O}_x\mathcal{A}_x^{-1})Q\sigma_yQ^t(\mathcal{A}_x\mathcal{O}_x\mathcal{A}_x^{-1}) \\ \tilde{\sigma}_y &= \sigma_y + (\mathcal{A}_y\mathcal{O}_y\mathcal{A}_y^{-1})Q\sigma_xQ^t(\mathcal{A}_y\mathcal{O}_y\mathcal{A}_y^{-1}). \end{aligned} \quad (39)$$

Note that the off diagonal blocks in $\tilde{\sigma}$ are linear in the phase advance matrices \mathcal{O}_x and \mathcal{O}_y and therefore vanish when averaging over the phases. This implies that the beam after filamentation is uncoupled but the respective 2×2 sigma matrices are affected.

The expressions for $\tilde{\sigma}_{x/y}$ can be evaluated in a straightforward, albeit tedious way and after averaging over the phases in the rotation matrices \mathcal{O}_x and \mathcal{O}_y we find

$$\tilde{\sigma} = \begin{pmatrix} \sigma_x + \frac{\varepsilon_y}{2\varepsilon_x} \frac{\beta_x\beta_y}{f^2} \sigma_x & 0_2 \\ 0_2 & \sigma_y + \frac{\varepsilon_x}{2\varepsilon_y} \frac{\beta_x\beta_y}{f^2} \sigma_y \end{pmatrix} \quad (40)$$

and after expressing the matched beam matrices σ_x and σ_y using eq. 2 we find the rms emittances $\tilde{\varepsilon}_{x/y}$ at the interaction point to be

$$\tilde{\varepsilon}_x = \varepsilon_x + \frac{\kappa^2}{2}\varepsilon_y \quad \text{and} \quad \tilde{\varepsilon}_y = \varepsilon_y + \frac{\kappa^2}{2}\varepsilon_x \quad (41)$$

where we introduced the coupling factor $\kappa = \beta_x \beta_y / f^2$. Remember that the beta function appearing in the definition of κ are those of the skew quadrupole and we find that the emittance growth is proportional to both beta-functions at the skew quadrupole and also proportional to inverse focal length, the strength, of the skew quadrupole. Equation 41 also tells us that the emittance of the orthogonal plane is projected into the plane. In this way it is obvious that the smaller emittance, usually the vertical, is worse affected by skew errors, because the larger horizontal emittance is added to it proportional to the coupling strength κ^2 .

The discussion so far only took into account the averaged effect on the rms emittances, but not the shape of the beam distribution after filamentation. This is what we address in the following paragraphs. We start by considering the matched beam distribution function just before the skew quadrupole

$$\psi(x, x', y, y') = \frac{1}{(2\pi)^2 \varepsilon_x \varepsilon_y} \exp \left[-\frac{1}{2} \sum_{i=1}^4 \sum_{j=1}^4 \bar{\sigma}_{ij}^{-1} x_i x_j \right] \quad (42)$$

where we introduce the notation x_i for $i = 1, \dots, 4$ denotes (x, x', y, y') for convenience. Note that the inverse of the beam matrix from eq. 33 appears in the argument of the exponential function.

The task at hand is now to calculate the distribution function after the skew quadrupole, introduce action-angle variables and then perform the phase averaging in order to calculate the distribution after filamentation at the interaction point. The inverse of the beam matrix before the skew quad is

$$\bar{\sigma}^{-1} = \begin{pmatrix} \frac{1}{\varepsilon_x} \begin{pmatrix} \gamma_x & \alpha_x \\ \alpha_x & \beta_x \end{pmatrix} & 0_2 \\ 0_2 & \frac{1}{\varepsilon_y} \begin{pmatrix} \gamma_y & \alpha_y \\ \alpha_y & \beta_y \end{pmatrix} \end{pmatrix} \quad (43)$$

and we now use this to calculate the inverse of the beam matrix after the skew quadrupole $\hat{\sigma}^{-1}$. Since $\hat{\sigma}$ is given by eq. 34 we can easily invert it by writing

$$\hat{\sigma}^{-1} = (S^t)^{-1} \bar{\sigma}^{-1} S^{-1} = \begin{pmatrix} 1_2 & Q^t \\ Q^t & 1_2 \end{pmatrix}^{-1} \bar{\sigma}^{-1} \begin{pmatrix} 1_2 & Q \\ Q & 1_2 \end{pmatrix}^{-1} \quad (44)$$

and some extensive algebra, where we use the fact the $Q^2 = 0_2$ with Q from eq. 35 and also

$$\begin{pmatrix} 1_2 & Q \\ Q & 1_2 \end{pmatrix}^{-1} = \begin{pmatrix} 1_2 & -Q \\ -Q & 1_2 \end{pmatrix}. \quad (45)$$

we arrive at the inverse after the skew quadrupole

$$\hat{\sigma}^{-1} = \begin{pmatrix} \sigma_x^{-1} + Q^t \sigma_y^{-1} Q & -\sigma_x^{-1} Q - Q^t \sigma_y^{-1} \\ -Q^t \sigma_x^{-1} - \sigma_y^{-1} Q & \sigma_y^{-1} + Q^t \sigma_x^{-1} Q \end{pmatrix} \quad (46)$$

such that the distribution after the skew quadrupole now looks like

$$\psi(x, x', y, y') = \frac{1}{(2\pi)^2 \varepsilon_x \varepsilon_y} \exp \left[-\frac{1}{2} \sum_{i=1}^4 \sum_{j=1}^4 \hat{\sigma}_{ij}^{-1} x_i x_j \right]. \quad (47)$$

Essentially, only $\bar{\sigma}$ was changed to $\hat{\sigma}$ in the argument of the exponent and $\hat{\sigma}$ is given by the previous equation.

In order to propagate this distribution further down the assumed uncoupled linac we introduce normalized phase space coordinates in four dimensions by

$$\begin{pmatrix} x \\ x' \\ y \\ y' \end{pmatrix} = \begin{pmatrix} \mathcal{A}_x & 0_2 \\ 0_2 & \mathcal{A}_y \end{pmatrix} \begin{pmatrix} \tilde{x} \\ \tilde{x}' \\ \tilde{y} \\ \tilde{y}' \end{pmatrix} \quad (48)$$

where the $\mathcal{A}_{x/y}$ are defined in eq. 1. If we want to express the argument of the exponential function in the variables of normalized phase space we need to calculate the inverse of the beam matrix $\tilde{\sigma}^{-1}$ in those variables and find

$$\tilde{\sigma}^{-1} = \begin{pmatrix} \mathcal{A}_x^t & 0_2 \\ 0_2 & \mathcal{A}_y^t \end{pmatrix} \hat{\sigma}^{-1} \begin{pmatrix} \mathcal{A}_x & 0_2 \\ 0_2 & \mathcal{A}_y \end{pmatrix} \quad (49)$$

with $\hat{\sigma}^{-1}$ given by eq. 46. Some more tedious algebra yields

$$\tilde{\sigma}^{-1} = \begin{pmatrix} \mathcal{A}_x^t \sigma_x^{-1} \mathcal{A}_x + \mathcal{A}_x^t Q^t \sigma_y^{-1} Q \mathcal{A}_x^t & -\mathcal{A}_x^t [\sigma_x^{-1} Q + Q^t \sigma_y^{-1}] \mathcal{A}_y^t \\ -\mathcal{A}_y^t [Q^t \sigma_x^{-1} + \sigma_y^{-1} Q] \mathcal{A}_x^t & \mathcal{A}_y^t \sigma_y^{-1} \mathcal{A}_y + \mathcal{A}_y^t Q^t \sigma_x^{-1} Q \mathcal{A}_y^t \end{pmatrix}. \quad (50)$$

Now all the terms can be evaluated individually with the result

$$\begin{aligned} \mathcal{A}_x^t \sigma_x^{-1} \mathcal{A}_x &= \frac{1}{\varepsilon_x} 1_2 \\ \mathcal{A}_x^t Q^t \sigma_y^{-1} Q \mathcal{A}_x^t &= \frac{1}{\varepsilon_y} \begin{pmatrix} \kappa^2 & 0 \\ 0 & 0 \end{pmatrix} \\ \mathcal{A}_x^t \sigma_x^{-1} Q \mathcal{A}_y &= \frac{1}{\varepsilon_x} \begin{pmatrix} 0 & 0 \\ \kappa & 0 \end{pmatrix} \\ \mathcal{A}_x^t Q^t \sigma_y^{-1} \mathcal{A}_y &= \frac{1}{\varepsilon_y} \begin{pmatrix} 0 & \kappa \\ 0 & 0 \end{pmatrix} \\ \mathcal{A}_y^t Q^t \sigma_x^{-1} \mathcal{A}_x &= \frac{1}{\varepsilon_x} \begin{pmatrix} 0 & \kappa \\ 0 & 0 \end{pmatrix} \\ \mathcal{A}_y^t \sigma_y^{-1} Q \mathcal{A}_x &= \frac{1}{\varepsilon_y} \begin{pmatrix} 0 & 0 \\ \kappa & 0 \end{pmatrix} \end{aligned} \quad (51)$$

where we use the definition of $\kappa^2 = \beta_x \beta_y / f^2$ from above. Inserting all terms into the expression for $\tilde{\sigma}^{-1}$ we obtain

$$\tilde{\sigma}^{-1} = \begin{pmatrix} \frac{1}{\varepsilon_x} + \frac{\kappa^2}{\varepsilon_y} & 0 & 0 & \frac{1}{\varepsilon_y} \\ 0 & -\frac{\kappa}{\varepsilon_x} & -\frac{\kappa}{\varepsilon_x} & 0 \\ 0 & -\frac{\kappa}{\varepsilon_x} & \frac{1}{\varepsilon_y} + \frac{\kappa^2}{\varepsilon_x} & 0 \\ -\frac{\kappa}{\varepsilon_y} & 0 & 0 & \frac{1}{\varepsilon_y} \end{pmatrix}. \quad (52)$$

Note that in the absence of coupling $\kappa = 0$ the matrix reverts to the matrix that contains the inverse emittances on the diagonal.

In order to express the distribution function in action-angle variables J and ϕ we change the variables according to

$$\tilde{z} = \begin{pmatrix} \tilde{x} \\ \tilde{x}' \\ \tilde{y} \\ \tilde{y}' \end{pmatrix} = \begin{pmatrix} \sqrt{2J_x} \cos \phi_x \\ \sqrt{2J_x} \sin \phi_x \\ \sqrt{2J_y} \cos \phi_y \\ \sqrt{2J_y} \sin \phi_y \end{pmatrix} \quad (53)$$

which lets us express the argument of the exponential function in the distribution function (apart from the factor 1/2) in the form

$$\begin{aligned} \tilde{z}^t \tilde{\sigma}^{-1} \tilde{z} &= \frac{2J_x}{\varepsilon_x} + \frac{2J_x \kappa^2}{\varepsilon_y} \cos^2 \phi_x - \frac{2\kappa}{\varepsilon_y} \sqrt{2J_x} \sqrt{2J_y} \cos \phi_x \sin \phi_y \\ &+ \frac{2J_y}{\varepsilon_y} + \frac{2J_y \kappa^2}{\varepsilon_x} \cos^2 \phi_y - \frac{2\kappa}{\varepsilon_x} \sqrt{2J_x} \sqrt{2J_y} \cos \phi_y \sin \phi_x \end{aligned} \quad (54)$$

and the distribution function in action angle variables can finally be written as

$$\begin{aligned} \psi(J_x, \phi_x, J_y, \phi_y) &= \frac{1}{(2\pi)^2 \varepsilon_x \varepsilon_y} \exp \left[-\frac{J_x}{\varepsilon_x} - \frac{J_y}{\varepsilon_y} - \frac{\kappa^2 J_x}{\varepsilon_y} \cos^2 \phi_x - \frac{\kappa^2 J_y}{\varepsilon_x} \cos^2 \phi_y \right] \\ &\times \exp \left[\frac{\kappa}{\varepsilon_y} \sqrt{2J_x} \sqrt{2J_y} \cos \phi_x \sin \phi_y \right. \\ &\quad \left. + \frac{\kappa}{\varepsilon_x} \sqrt{2J_x} \sqrt{2J_y} \cos \phi_y \sin \phi_x \right]. \end{aligned} \quad (55)$$

The effect of filamentation is, similar to what we did in the simple cases in previous sections, given by the phase average over the angle variables ϕ_x and ϕ_y and we calculate

$$\langle \psi(J_x, J_y) \rangle_{\phi_x, \phi_y} = \frac{1}{(2\pi)^2} \int_{-\pi}^{\pi} \int_{-\pi}^{\pi} \psi(J_x, \phi_x, J_y, \phi_y) d\phi_x d\phi_y \quad (56)$$

which, unfortunately, we were unable to solve analytically. It is, however, straightforward to evaluate the integral numerically on a grid of values for J_x and J_y for

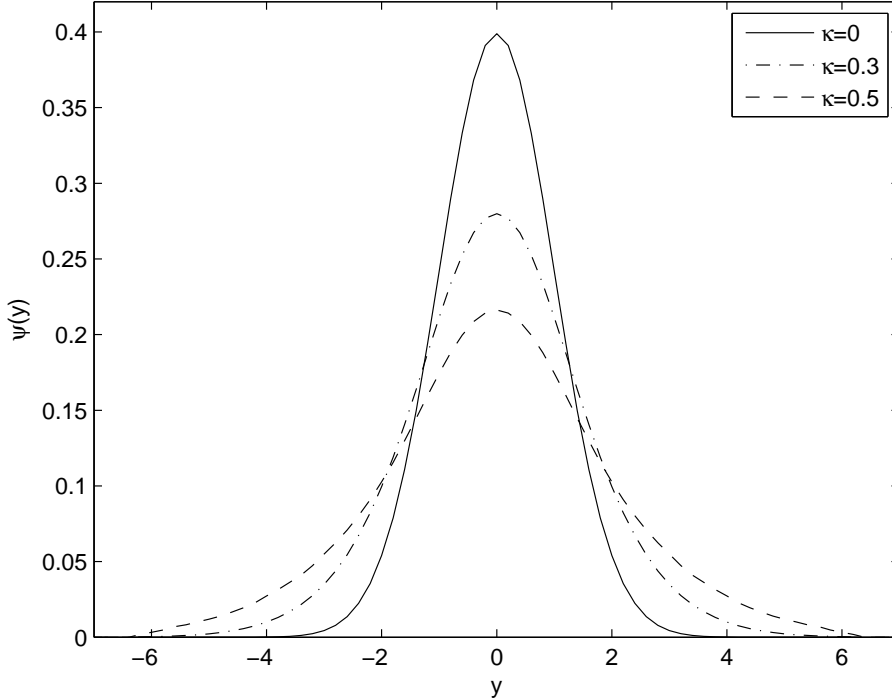


Figure 6: The normalized vertical distribution for $\varepsilon_x/\varepsilon_y = 30$ and $\kappa = 0.0, 0.3$ and 0.5 .

given parameters $\varepsilon_x, \varepsilon_y$, and κ . We chose to normalize the variables J_x, J_y , and ε_x to the vertical emittance ε_y which we consequently set to unity.

In order to calculate the luminosity degradation as a function of the coupling κ for different emittance ratios $\varepsilon_x/\varepsilon_y = 10, 20, \dots, 50$ we use the phase-averaged distribution that is defined on the grid, and express the action variables J_x and J_y by 'new' variables $\tilde{x}, \tilde{x}', \tilde{y}, \tilde{y}'$ in normalized phase space $J_x = (\tilde{x}^2 + \tilde{x}'^2)/2$ and the corresponding expression for the vertical plane. Note, that this is the normalized phase space *after* filamentation which is different from the phase space used in eq. 53 despite our use of the same symbols for the variables.

The resulting distribution function is now a function of the 'new' normalized phase space variables and the spatial distribution can be calculated by numerically by integrating over the angle variables \tilde{x}' and \tilde{y}' which determine the action variables $J_x = (\tilde{x}^2 + \tilde{x}'^2)/2$ and $J_y = (\tilde{y}^2 + \tilde{y}'^2)/2$ that determine the value of the distribution function ψ by interpolating on the grid. This procedure results in a distribution function $\psi_\kappa(\tilde{x}, \tilde{y})$ which describes the spatial distribution of the beam, expressed in variables of the 'new' normalized phase space after filamentation. It is instructive to display the vertical distribution, which is obtained by

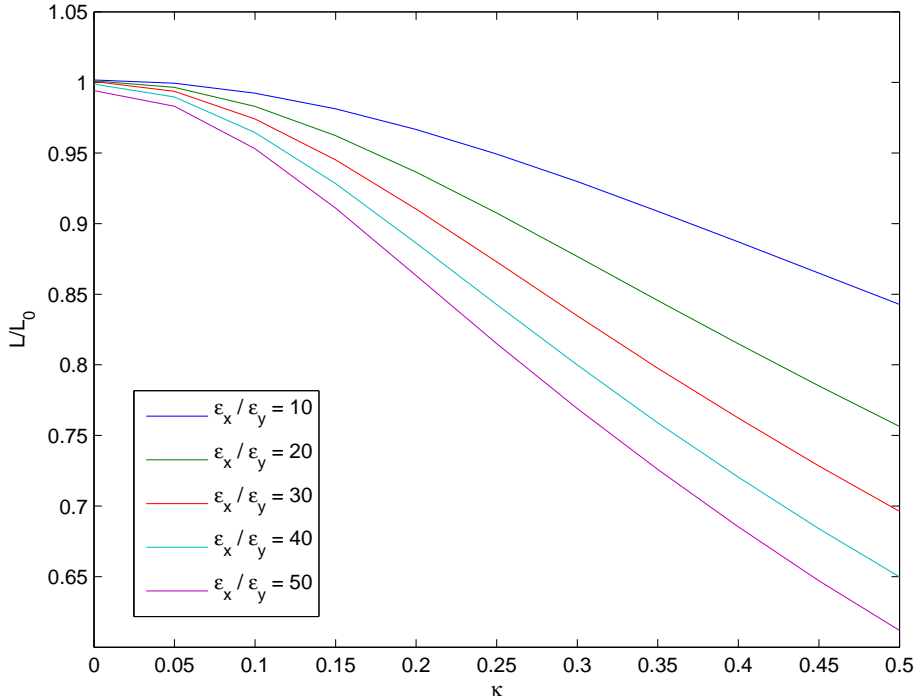


Figure 7: The luminosity loss as a function of the coupling parameter κ for different emittance ratios ϵ_x/ϵ_y .

numerically integrating once more over \tilde{x} which is shown in Fig. 6 for an emittance ratio $\epsilon_x/\epsilon_y = 30$ and for $\kappa = 0, 0.2, 0.5$. We observe the expected widening of the distribution, which comes from projecting the large horizontal emittance onto the vertical plane.

The geometric luminosity is proportional to the spatial overlap integral of the distribution with a given value of κ with the distribution of the counter-propagating beam, that we assume to be the unperturbed one, which corresponds to $\kappa = 0$.

$$\mathcal{L} \propto \int_{-\infty}^{\infty} \int_{-\infty}^{\infty} \psi_0(\tilde{x}, \tilde{y}) \psi_{\kappa}(\tilde{x}, \tilde{y}) d\tilde{x} d\tilde{y} . \quad (57)$$

In the following we will characterize the loss of geometric luminosity by normalizing with respect to the overlap integral of two unperturbed distributions $\psi_0(\tilde{x}, \tilde{y})$. The unperturbed distributions are pure Gaussians, characterized by ϵ_x and ϵ_y , and the integral can be evaluated analytically with the result $\mathcal{L}_0 \propto 1/4\pi\epsilon_x\epsilon_y$. In Fig. 7 we show the relative geometric luminosity loss $\mathcal{L}/\mathcal{L}_0$ as a function of the coupling perturbation κ for emittance ratios $\epsilon_x/\epsilon_y = 10, 20, \dots, 50$. We find, not surprisingly, that the luminosity decreases with increasing coupling and that the effect is worse for larger emittance ratios ϵ_x/ϵ_y . A coupling factor of $\kappa = 0.1$

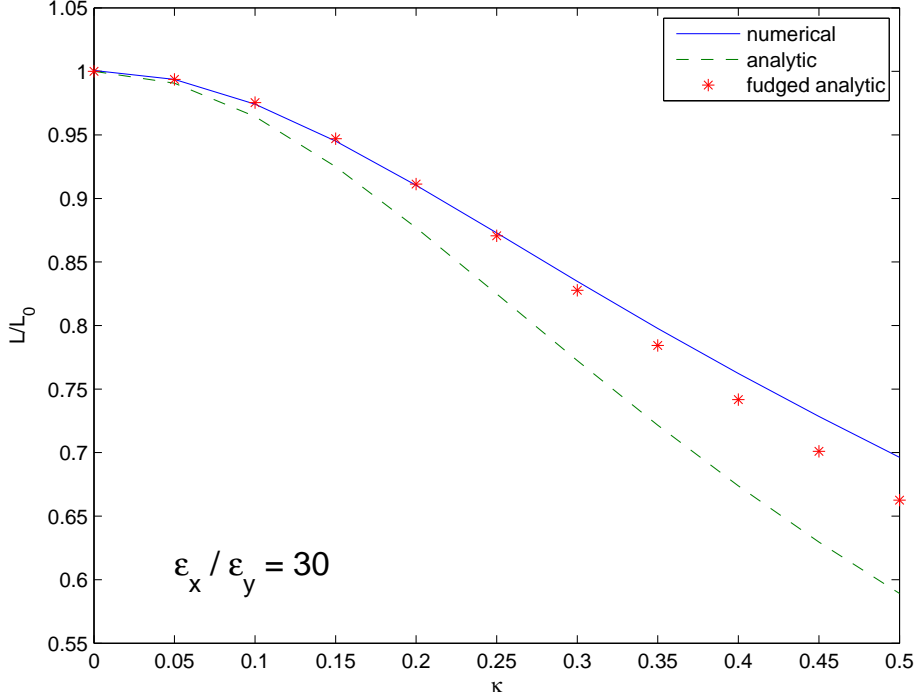


Figure 8: Comparison of the approximations for the luminosity loss given in eq. 58 (dashed) and eq. 59 (asterisks) with the numerically evaluated values (solid).

results in reductions of 0.9 %, 1.8 %, 2.7 %, 3.4 %, and 4.1 %, respectively for the different emittance ratios.

It is interesting to compare the luminosity loss \mathcal{L} calculated using the proper distribution with the luminosity \mathcal{L}^g derived from convoluting a Gaussian distribution whose rms is given by eq. 41 for the corresponding value of κ . The latter can be calculated by averaging two Gaussians and we obtain

$$\mathcal{L}^g/\mathcal{L}_0 = \frac{1}{\sqrt{1 + (1/2)\kappa^2\varepsilon_y/\varepsilon_x}} \frac{1}{\sqrt{1 + (1/2)\kappa^2\varepsilon_x/\varepsilon_y}} \quad (58)$$

In Fig. 8 we display the proper numerical luminosity loss for $\varepsilon_x/\varepsilon_y = 30$ as a blue solid line and the luminosity emittance loss from eq. 58 as a green dashed line. We find that the emittance loss based on eq. 58 overestimates the loss. By empirically tuning the parameter 1/2 in front of the κ^2 terms to 0.34 results in the red asterisks in Fig. 8 and yields a much improved approximation of the proper numerical result shown as the solid line.

The reason for the improved approximation by the empirically found parameter can be understood by plotting the spatial projection onto the vertical axis

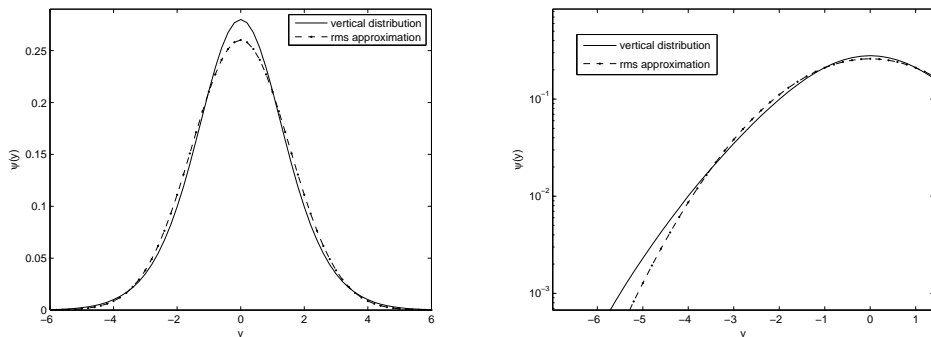


Figure 9: The vertical distribution for $\varepsilon_x/\varepsilon_y = 30$ and $\kappa = 0.3$ is shown as a solid line and the approximation based on eq. 41 is shown as a dashed line. From the right plot, which shows the same data on a logarithmic scale, we see that the tail of the solid is larger than the dashed distribution. This leads to an overestimate of the rms value on which eq. 41 is based.

of the proper distribution and the Gaussian approximation, which is shown in the left plot in Fig. 9. We observe that the approximation is smaller near the center, and is larger in the tails of the distribution. The latter is visible on the right plot, which shows the distribution on a logarithmic scale. Larger values in the tails causes the rms to be biased to a larger value. We conclude that the following heuristic equation may serve as a suitable approximation to estimate the luminosity loss from filamentation caused by coupling errors

$$\mathcal{L}/\mathcal{L}_0 = \frac{1}{\sqrt{1 + 0.34\kappa^2\varepsilon_y/\varepsilon_x}} \frac{1}{\sqrt{1 + 0.34\kappa^2\varepsilon_x/\varepsilon_y}}. \quad (59)$$

We need to point out that we tested the approximation also for the other emittance ratios in Fig. 7 with good success, at least up to $\kappa \approx 0.3$.

6 CLIC

In Ref. [4] the effect of RF-breakdown in the accelerating structures of CLIC on the beam is discussed and the quoted values for their magnitude are

- Transverse kick: $\theta \approx 29$ keV
- Focal length: $f \approx 5$ m at 180 MeV electron energy
- Energy loss: $\Delta E \approx 23$ MeV

where the energy loss corresponds to one non-contributing accelerating structure, because the breakdown created a plasma that reflects the incident RF.

Part of the discussed analysis was used in ref. [10] to estimate the effect of breakdown on the CLIC beam. There it was found that the effect is most severe at the injection energy, where vertical kicks can have magnitude above 10 times the angular divergence, leading to an annular beam that reduces the luminosity by as much as a factor of 10 as is obvious from Fig. 3. The effect of energy loss was found to be negligible.

The focal length found to be 5 m at 180 MeV scales to about 250 m at 9 GeV injection energy, which makes the factors describing the emittance increase rather small. Assuming beta-functions on the order of 10 m we find $\beta^2/2f^2$ for quadrupolar errors and $\beta_x\beta_y/f^2$ for skew quadrupolar errors to be on the order of a few times 10^{-3} . This leads to negligible luminosity loss according to Fig. 5 and Fig. 7.

7 Conclusions

We discussed the effect of perturbations to the beam due to RF-breakdown on the geometric luminosity. We modeled the effect by assuming that the perturbations fully filament during the passage of the beam along the linear accelerator and calculated the emittance increase as well as the shape of the resulting filamented distribution at the interaction point. Based on the well-known results for transverse kicks and beta-function mismatch as well as the, to our knowledge, new result for skew quadrupolar mismatch we used the filamented distributions at the interaction point to convolute them with the beam traveling in the opposite direction and derived luminosity loss functions for the different perturbations.

For CLIC parameters we found that the most significant perturbations are vertical kicks at the beginning of the linear accelerator where the beam energy is still comparatively low. Quadrupolar errors from upright and skew-quadrupoles are less important.

The application of the mismatch formulae is not limited to the determination of luminosity loss. Injection errors into a ring will equally filament out and lead to an increased beam phase space, whose spatial profiles are given by those shown in Fig. 2, 4 and 6. Moreover, static errors, such as stray fields incorrectly set power supplies for dipoles and quadrupoles in the accelerator can be treated in the same way.

Support from the Swedish Research Council, contract 2014-6360 is acknowledged.

References

- [1] S. Stapnes (Ed.), *The CLIC Programme: Towards a Staged e+e- Linear Collider Exploring the Terascale*, CERN-2012-005, Geneva, 2012.

- [2] M. Johnson, R. Ruber, V. Ziemann, H. Braun, *Arrival time measurements of ions accompanying RF breakdown*, Nucl. Inst. and Methods A 595 (2008) 568.
- [3] A. Dubrovskiy et al., *Flashbox Compact Beam Spectrometer and its Application to the High-gradient Acceleration Study*, Proceedings of the 4th International Particle Accelerator Conference, Shanghai, China, May 2013.
- [4] A. Palaia, et. al, *Effects of rf breakdown on the beam in the Compact Linear Collider prototype accelerator structure*, Physical Review Special Topics - Accelerators and Beams, 16, 081004 (2013).
- [5] T. Raubenheimer, F.-J. Decker, J. Seeman, *Beam distribution function after filamentation*, SLAC-PUB-6850, Proceedings of the 1995 Particle Accelerator Conference and International Conference on High - Energy Accelerators, Piscataway, NJ, IEEE, 1996.
- [6] M. Syphers, *Injection Mismatch and Phase Space Dilution*, FERMILAB-FN-0458, 1987.
- [7] M. Abramowitz, I. Stegun, *Handbook of Mathematical Functions*, Dover, New York, 1972.
- [8] W. Fischer, *An Experimental study on the long term stability of particle motion in hadron storage rings*, DESY-95-235.
- [9] F.-J. Decker, et al., *Dispersion and betatron matching into the Linac*, Proceedings of the 1991 Particle Accelerator Conference, San Francisco, 1991.
- [10] A. Palaia, *Beam Momentum Changes due to Discharges in High-gradient Accelerator Structures*, Doctoral thesis, Uppsala University, December 2013. URN: urn:nbn:se:uu:diva-208567